



Dynamics of Short Recoil-Operated Weapon

Martin MACKO^{1*}, Bien Van VO², Quang Anh MAI²

¹University of Defence, Faculty of Military Technology,
65 Kounicova Str., 662 10 Brno, Czech Republic

²Le Quy Don Technical University,
236 Hoang Quoc Viet, Hanoi, Vietnam

*Corresponding author's e-mail address and ORCID:
martin.macko@unob.cz; <https://orcid.org/0000-0002-3896-0803>

Received: February 19, 2021 / Revised: April 6, 2021 / Accepted: May 4, 2021 /
Published: September 30, 2021

DOI 10.5604/01.3001.0015.2432

Abstract. In this article, the authors mentioned the function of short-recoil-operated weapons with a vertical sliding-wedge breechblock. The dynamic simulation was conducted and then the results were compared with the corresponding experimental data to verify reliability of the model. The model is calculated and tested out on the 37 mm twin anti-aircraft gun. Besides, the article presents the effect of some structural parameters on functionality of the automatic weapon. The reported results are an important theoretical basis to determine the rate of fire and the forces acting on the guns. The movement of the breechblock also affects stability of the weapon and can therefore be used to a math model or to simulate the movement of the weapon. Calculated and verified data could be used for the design of an automatic firing system as well as for solving vibration on automatic guns when burst firing.

Keywords: dynamics, short-recoil-operated weapons, Lagrange's equations

1. INTRODUCTION

A selected principle of breech moving plays the key role for weapon design. Its kinetic characteristics have the direct bearing on the stability of the whole system. Based on the principle of using propellant gas energy, automatic weapons are divided into 3 types: mass locked weapons (so called blowback weapons), recoil-operated weapons, and gas-operated weapons, see [1], [2] and [3]. Calculating automatic weapon dynamics is one of important tasks in the process of designing as well as exploiting automatic guns and it is different for each type of automatic weapon. An aim of this calculation is determination of the rate of fire (cadence), the movement of recoiling parts, forces acting on the breech casing, and the mounting. Results of this calculation are input data for solving stability and vibration on automatic guns.

The main purpose of this paper is not only to clarify the basis of the calculation but also to present calculation steps, the results of dynamic calculation of short recoil-operated weapon with the vertical sliding-wedge breechblock. The results are applied on 37 mm twin anti-aircraft gun K65 (Fig. 1), see [4], [5] and compared by experimental measurement.

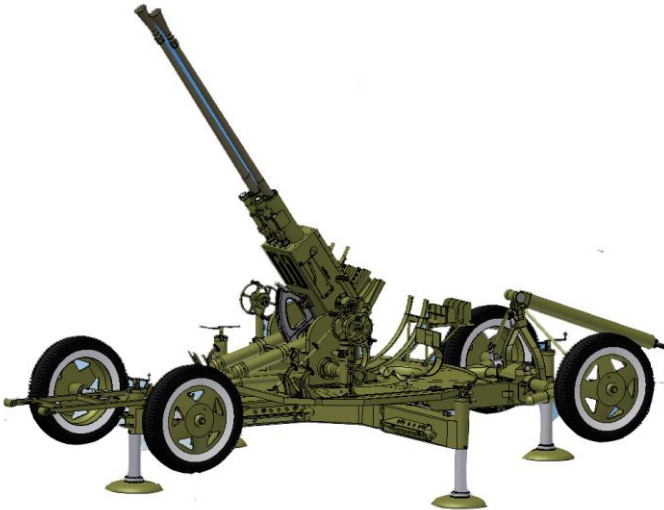


Fig. 1. Overview of 37 mm K65 twin-barrel anti-aircraft gun

2. PROBLEM FORMULATION

2.1. Model of recoil-operated weapon

To build the system of differential equations of automatic machine gun movement, several assumptions are used as follows:

- springs are elastic detail; automatic movement system's other parts are absolute solid objects,
- planar kinematics is used,
- the mass of objects is placed at the centre of the object or at the centre of gravity,
- the effect of the gap between dynamic joints is ignored.

A gun automatic mechanism consists of a basic mechanism with the mass m_0 and working mechanisms with the mass m_i . The angle α_i presents a motion direction of the i -th working mechanism with the basic mechanism. The parameter k_i is the transmission ratio and η_i is power from the basic mechanism to the i -th working mechanism. The physical model of a gun automatic system is given in Fig. 2.

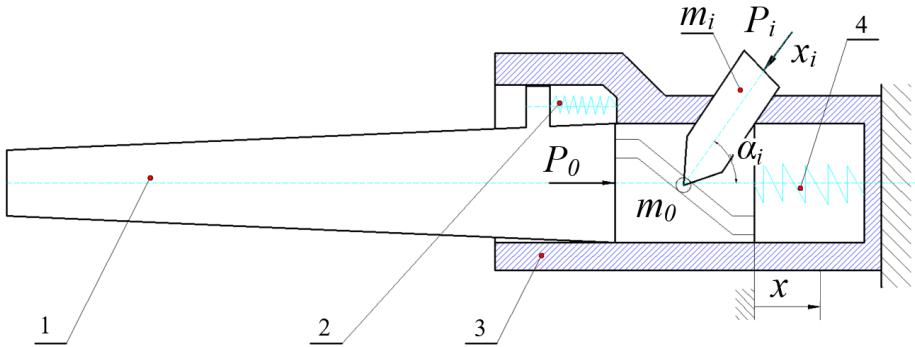


Fig. 2. A short recoil system scheme of a gun automatic firing system:
 1. Recoiling parts; 2. Barrel spring; 3. Receiver; 4. Rammer spring

Differential equations of automatic system motion can be obtained by using the d'Alembert's principle of a dynamic mechanical analysis for each part, using the Newton's second law of motion or using the Lagrange's equations. Because the automatic firing system contains kinetic binding, the Lagrange's equation is used in this paper, see [6], [7], and [8]:

$$\frac{d}{dt} \left(\frac{\partial T}{\partial \dot{q}_j} \right) - \frac{\partial T}{\partial q_j} + \frac{\partial \Pi}{\partial q_j} = Q_j \quad (j=1, 2, \dots) \quad (1)$$

where: T – total kinetic energy of the mechanical system;

Π – the potential energy of the system;

q_j – independent generalised coordinate;

Q_j – generalised force corresponding to the generalised coordinates q_j ,

j – degrees of freedom.

Corresponding to the model in Fig. 2, the mechanical system has only the independent generalised coordinate $q_1 = x$, displacement of the basic mechanism compared to the receiver.

The kinetic energy of a mechanical system is determined by the following formula:

$$T = \frac{m_0 V^2}{2} + \sum_{i=1}^n \frac{m_i V_i^2}{2} \quad (2)$$

where: V – absolute velocity of basic mechanism compared to the receiver,
 V_i – absolute velocity of the i -th working mechanisms compared to the receiver.

When the absolute velocity is represented through a generalised coordinate, we obtain:

$$\begin{aligned} V^2 &= \dot{x}^2; \\ V_i^2 &= \dot{x}_i^2 = k_i^2 \dot{x}^2 \end{aligned} \quad (3)$$

Substituting equations (3) into equation (2):

$$T = \frac{1}{2} \left(m_0 + \sum_{i=1}^n k_i^2 m_i \right) \dot{x}^2 \quad (4)$$

On the other hand, the transmission ratio k_i is a function of the basic mechanism displacement x . The next step is a calculation of the partial differential equation:

$$\begin{aligned} \frac{\partial T}{\partial x} &= \dot{x}^2 \sum_{i=1}^n k_i m_i \frac{\partial k_i}{\partial x}; \\ \frac{\partial T}{\partial \dot{x}} &= \left(m_0 + \sum_{i=1}^n k_i^2 m_i \right) \dot{x}; \\ \frac{d}{dt} \left(\frac{\partial T}{\partial \dot{x}} \right) &= \left(m_0 + \sum_{i=1}^n k_i^2 m_i \right) \ddot{x} + 2\dot{x}^2 \sum_{i=1}^n \frac{\partial k_i}{\partial x} m_i k_i \end{aligned} \quad (5)$$

The potential energy of the system:

$$\Pi = \Pi_o x + \frac{1}{2} c_0 x^2 \quad (6)$$

in which: c_0 – is the equivalent stiffness of return spring.

$$\frac{\partial \Pi}{\partial x} = \Pi_o + c_0 x \quad (7)$$

The generalised force is determined:

$$Q_1 = P_0 - \sum_{i=1}^n k_i P_i - \left(\sum_{i=1}^n F_{0i} + \sum_{i=1}^n k_i F_i \right) \quad (8)$$

where: P_0 – generalised force effects on basic mechanism;

P_i – generalised force effects on the i -th working mechanism;

F_i – friction force effects on the i -th working mechanism while effecting on basic mechanism;

F_{0i} – friction force effects on basic mechanism in position associated with the i -th working mechanism.

Friction Force Calculation F_{0i} and F_i

The Lagrange equation of the second kind is correct for an ideal mechanical binding system. In fact, the system transfers energy from the basic mechanism to the working mechanism under the simultaneous action of a frictional force, and thus energy is lost. The friction force is determined as follows, see Fig. 3:

$$\eta_i = \frac{R_i}{R_0} k_i \quad (9)$$

where: R_0 – actuation force is applied to the basic mechanism,

R_i – drag force is applied to the working mechanism.

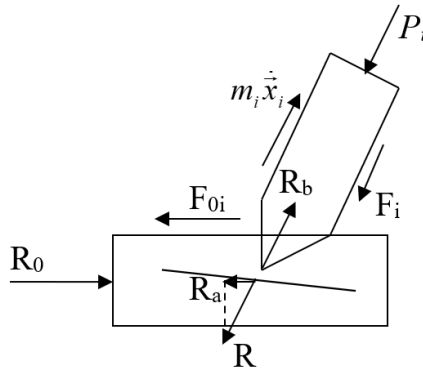


Fig. 3. Force exerted on the basic mechanism and working mechanisms

Equations are valid:

$$R_0 = R_a + F_{0i} \quad (10)$$

$$R_i = R_b - F_i \quad (11)$$

where: R_a, R_b – the projection of a reactive force into the direction of motion,
 F_{0i}, F_i – the projection of a friction force into the direction of motion.

The drag force is applied to the i -th working mechanism:

$$R_i = m_i \frac{d\dot{x}_i}{dt} + P_i \quad (12)$$

where: \dot{x}_i – velocity of the i -th working mechanism.

In the case of n the working mechanisms, we obtain:

$$\sum_{i=1}^n R_{0i} = \sum_{i=1}^n R_a + \sum_{i=1}^n F_{0i} \quad (13)$$

Substituting equations (9) and (12) into equation (13):

$$\sum_{i=1}^n \frac{k_i}{\eta_i} \left(m_i \frac{d\dot{x}_i}{dt} + P_i \right) = \sum_{i=1}^n R_a + \sum_{i=1}^n F_{0i} \quad (14)$$

Through the transformation, we get:

$$\sum_{i=1}^n F_{0i} + \sum_{i=1}^n k_i F_i = \sum_{i=1}^n k_i \left(\frac{1}{\eta_i} - 1 \right) \left(m_i \frac{d\dot{x}_i}{dt} + P_i \right) \quad (15)$$

Substituting equation (15) into equation (8) and transforming, the generalised force is determined as follow:

$$Q_1 = P_0 - \sum_{i=1}^n \frac{k_i}{\eta_i} P_i - \sum_{i=1}^n k_i m_i \left(\frac{1}{\eta_i} - 1 \right) \left(\dot{x}^2 \frac{dk_i}{dx} + k_i \ddot{x} \right) \quad (16)$$

Substituting equations (5), (7) and (16) into equation (1) and through transform, we obtain a motion differential equation of the following form:

$$M_{11} \ddot{x} + M_{qt} \dot{x}^2 + c_0 x = P_1 \quad (17)$$

where:

$$\begin{aligned} M_{11} &= m_0 + \sum_{i=1}^n \frac{k_i^2}{\eta_i} m_i; \\ M_{qt} &= \sum_{i=1}^n \frac{k_i}{\eta_i} m_i \frac{dk_i}{dx}; \\ P_1 &= P_0 - \Pi_0 - \sum_{i=1}^n \frac{k_i}{\eta_i} P_i \end{aligned} \quad (18)$$

2.2. Mathematical model for the 37 mm twin anti-aircraft gun-type 65

37 mm twin anti-aircraft gun type 65 is automatic firing system operating on the short recoil principle; a vertical sliding-wedge breech block is produced in China. Recoiling parts include the barrel, return spring of the recuperator, breech ring, breech mechanism, cartridge ramming mechanism and the piston rod of the recoil cylinder assembly. It is a base link of an automatic firing system in the whole motion, see Fig. 4.

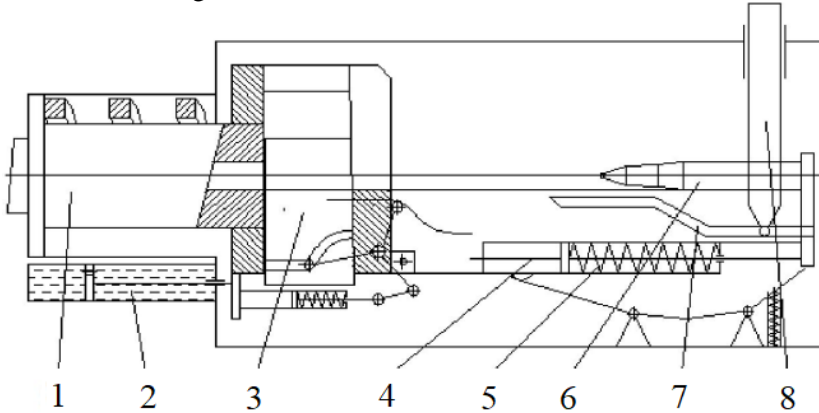


Fig. 4. Recoiling parts of a machine gun

1. Barrel assembly; 2. Recoil mechanism; 3. Breech; 4. Rammer shoe; 5. Rammer spring; 6. Cartridge; 7. Cam groove; 8. Feed rod

Applying the motion equation of the automatic firing system (17) above, we obtain the motion differential equation of the 37 mm twin anti-aircraft gun-type 65 as follows:

- in recoil,

$$\left(M_0 + \xi_i \sum_{i=1}^n m_i \frac{k_i^2}{\eta_i} \right) \dot{V} + \xi_i M_{qt} V^2 = P_{lg} + \xi_i \sum_{i=1}^n \frac{k_i}{\eta_i} P_i - R_{HL} \quad (19)$$

- in counter-recoil,

$$\left(M_0 + \xi_i \sum_{i=1}^n m_i \frac{k_i^2}{\eta_i} \right) \dot{V}_A + \xi_i M_{qt} V_A^2 = \Pi - R \quad (20)$$

where: M_0 – the mass of recoiling parts;

P_{lg} – the propellant gases' pressure force;

R_{HL} – the recoil braking force;

V – velocity of recoiling parts when in recoil;

V_A – velocity of recoiling parts when in counter-recoil;

M_{qt} – the extra inertia mass of the working mechanisms;

m_i, k_i, η_i – respectively is the mass, transmission ratio, and performance of the working mechanism i -th, respectively;

Π – recoil spring force;

R – total drag force while counter-recoil;

ξ_i – the control variable, equals 1 when the i -th dynamic binding joins the base and zero when the binding leaves.

The forces acting on the basic mechanism are included:

2.2.1. The propellant gases' pressure force (P_{lg})

Propellant gases' pressure force, acting on the barrel, is determined by the known pressure curve in the barrel which is the result of solution of the internal ballistics. According to the [9], the P_{lg} force is presented as follows:

$$P_{lg} = \frac{SP}{\varphi} \left(1 + \frac{0.5\omega}{q} \right) \quad (21)$$

where: S – inner cross section of the barrel;

φ – coefficient of secondary works account;

P – the average pressure of powder gas in the barrel;

ω, q – the mass of powder charge and bullet weight.

The aftereffect of gases, the propellant gases' pressure force is calculated using the approximate formula:

$$P_{lg} = p_d e^{-\frac{t}{b}} \quad (22)$$

$$b = \frac{(\beta - 0.5)\omega V_0}{g(p_d - p_k)} \quad (23)$$

where: p_d – gas pressure at the muzzle;

β – effect coefficient of propellant gases;

p_k – barometric pressure;

V_0 – muzzle velocity.

2.2.2. The recoil braking force (R_{HL})

The recoil braking force is determined as below, see [2]:

$$R_{HL} = \Phi_L + \Pi_{lx} + R_f - Q_0 \sin \varphi \quad (24)$$

where:

- $\Phi_L = f(a) \cdot V^2$: hydraulic resistance of the recoil mechanism;

$$\Phi_L = \frac{K\gamma}{2g} \left[\left(\frac{A_1 - A_v}{a_x} + 1 \right) (A_1 - A_v) + \frac{K_3 A_d^3}{K \Omega^2} \right] \cdot V^2 \quad (25)$$

V – velocity of barrel assembly;

$f(a_x)$ – the dependence of the hydraulic drag force in the recoil mechanism Φ_L with the area of the main flow hole a_x ;

K – correction coefficient of main flow drags;

γ – density of the liquid,

g – gravitational acceleration;

A_v – area of the throttling ring;

Ω – area of the auxiliary flow;

K_3 – correction coefficient of auxiliary flow drags;

A_1 – the working surface area of the piston when the barrel assembly pushed backward, is determined by the following formula:

$$A_1 = \frac{\pi}{4} (D^2 - d^2) \quad (26)$$

D – inside diameter of recoil cylinder,

d – outside diameter of piston rod.

A_d – working surface area of inner rolling chamber:

$$A_d = \frac{\pi}{4} d_1^2 \quad (27)$$

d_1 – inside diameter of a piston rod.

a_x – area of the main flow hole:

$$a_x = \frac{\pi}{4} (d_v^2 - \delta_{cdt}^2) \quad (28)$$

d_v – throttling ring diameter,

δ_{cdt} – controlling rod diameter.

- Π_{lx} : recoil spring force is opposite direction to the axis of recoil stroke. Its value is given by:

$$\Pi_{lx} = \Pi_0 + c_{lx} X \quad (29)$$

Π_0 – initial compression force of the recoil spring;

c_{lx} – stiffness of recoil spring;

X – displacement of the recoiling parts.

- R_f : friction force from the cradle slide parts to the recoiling part, is determined by the following formula:

$$R_f = Q_0 (f \cdot \cos \varphi + v) \quad (30)$$

Q_0 – gravity of recoiling part;

φ – elevation angle;

f – friction coefficient from cradle to recoiling brake;

v – friction coefficient from recoiling brake to obturator.

The graph of the recoil braking force of the 37 mm twin anti-aircraft gun type 65 is given in Fig. 5.

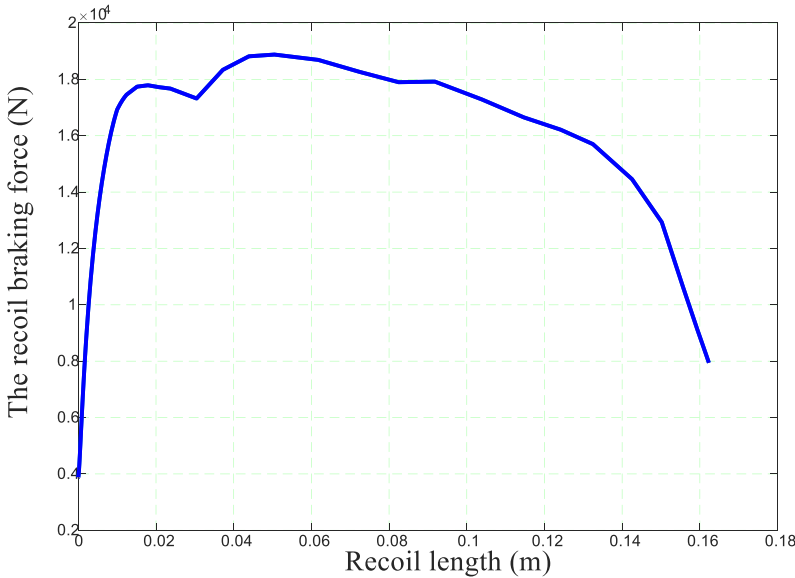


Fig. 5. The graph of the recoil braking force

2.2.3. Total drag force while counter-recoil (R)

The total drag force while counter-recoil is determined as below:

$$R = \Phi_{dl} + \Phi_{hd} \quad (31)$$

where:

- Φ_{dl} – the resistance counter-recoil force in recoil cylinder assembly: in counter-recoil, recoil cylinder assembly involved in the resistance counter-recoil process and the resistance counter-recoil force in recoil cylinder assembly is determined by the following formula:

$$\Phi_{dl} = \frac{K\gamma}{20g} \cdot \frac{A_2^3}{a_x^2} \cdot U^2 = f_{dl}(a_x) \cdot U^2 \quad (32)$$

- K – correction coefficient of main flow drags,
 γ – density of the liquid,
 U – velocity in counter-recoil,
 a_x – the area of the main flow hole is determined the same recoiling parts in recoil,
 A_2 – the working surface area in counter-recoil:

$$A_2 = \frac{\pi}{4} (D^2 - d_v^2) \quad (33)$$

- Φ_{hd} – the resistance counter-recoil force in a valve seat: The anti-aircraft gun requires a high rate of fire, so the counter-recoil is very fast, to avoid the cannon colliding with the cradle and to ensure slight upward movement. So, it is necessary to have the valve seat and the resistance counter-recoil force in the valve seat is determined as follows:

$$\Phi_{hd} = \frac{K_3 \gamma}{20g} \cdot \frac{A_d^3}{a_d^2} \cdot U^2 = f_{hd}(a_d) \cdot U^2 \quad (34)$$

- K_3 – correction coefficient of auxiliary flow drags,
 A_d – the working surface area of the inner rolling chamber,
 a_d – a total of the working surface area of the inclined hole. It can be written as follows:

$$a_d = n \cdot b \cdot h \quad (35)$$

- n – number of inclined holes,
 b – the inclined hole width,
 h – the depth of the inclined hole varies with the length of the control rod.

3. SIMULATION RESULTS ANALYSIS AND EXPERIMENTAL VERIFICATION

3.1. Applying Model to the 37 mm Twin Anti-Aircraft Gun Type 65

To solve the automatic firing system's problem, first, we need to define the system's input parameters. Parameters of mass and size are measured directly on the gun or are taken from design documents. Parameters of the moment of inertia, force set point, and centre of gravity coordinates were determined by Inventor software. Input parameters of the system are determined in [4], due to the very large number of inputs only the most important parameters are mentioned hereto, see Tab. 1.

Table 1. The input parameters of the system

Description	Symbol	Value
Calibre of gun	d	0.037 m
Weight of powder charge	ω_t	2.1 N
Initial volume of combustion chamber	W_0	$0.263 \cdot 10^{-3} \text{ m}^3$
Displacement of projectile inside the barrel	l	2.1 m
Cross-sectional area of bore barrel	S	$0.11 \cdot 10^{-2} \text{ m}^2$
Specific energy of powder	f	$95 \cdot 10^3 \text{ Nm/kg}$
Loading density of powder	Δ	7800 N/m^3
Co-volume of powder gas	α	$10^{-4} \text{ m}^3/\text{N}$
Total pressure impulse	I_k	$61 \cdot 10^4 \text{ Ns/m}^2$
Stiffness of return spring	c_{tx}	25500 N/m
Initial compression force of the return spring	II_0	3500 N
Gravity of recoiling part	Q_0	1300 N
Stiffness of rammer spring	C_r	313 N/m
Initial compression force of the rammer spring	P_r	51 N
Weight of the breech	Q_{kn}	67 N
Diameter of piston	d_{tt}	0.7 m
Throttling ring diameter	d_v	0.0245 m
Friction coefficient from cradle to recoiling brake	f	0.15
Friction coefficient from recoiling brake to obturator	v	0.3
Correction coefficient of main flow drags	K	1.1
Gravitational acceleration	g	9.81 m/s^2

To obtain accurate results, we combine the automatic firing system differential equation (19) and (20) with internal ballistic equations. The differential equations are solved by using the Runge-Kutta method and the MATLAB environment, the calculated results are shown in Fig. 6, 7 and Fig. 8.

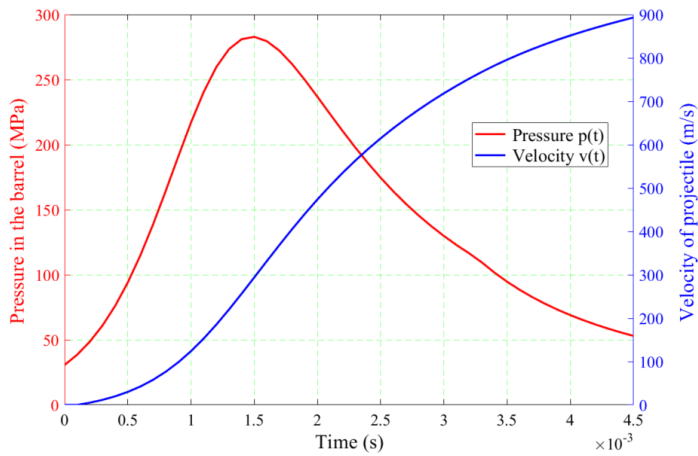


Fig. 6. Graph of pressure and velocity of a projectile

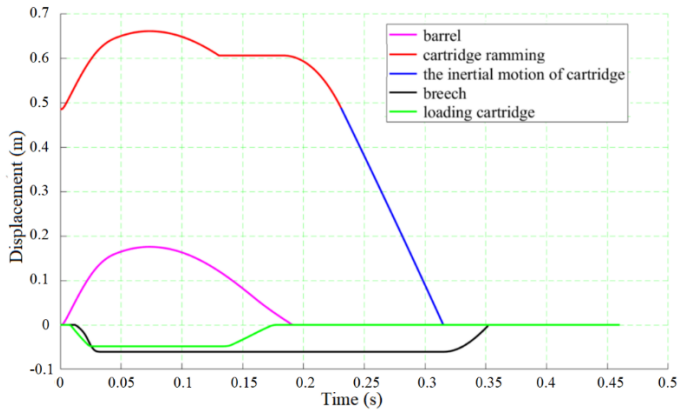


Fig. 7. Graph of the position of different parts of the automatic firing system

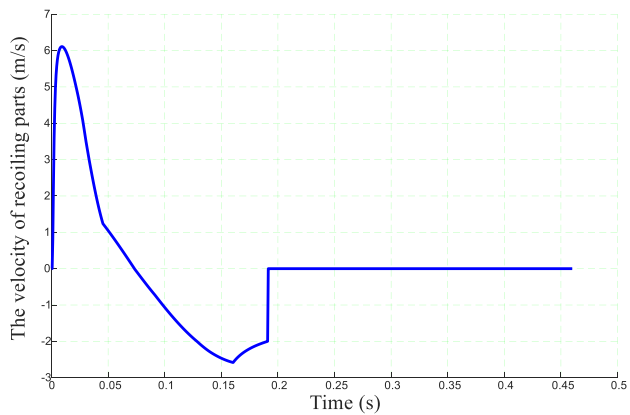


Fig. 8. Graph of velocity of recoiling parts

3.2. Assessing the Reliability of the Established Model

During the experimental part of the research, we have been used the contactless measurement techniques of the recoiling part displacement, using one high-speed camera, see positions 3 in Fig. 9.

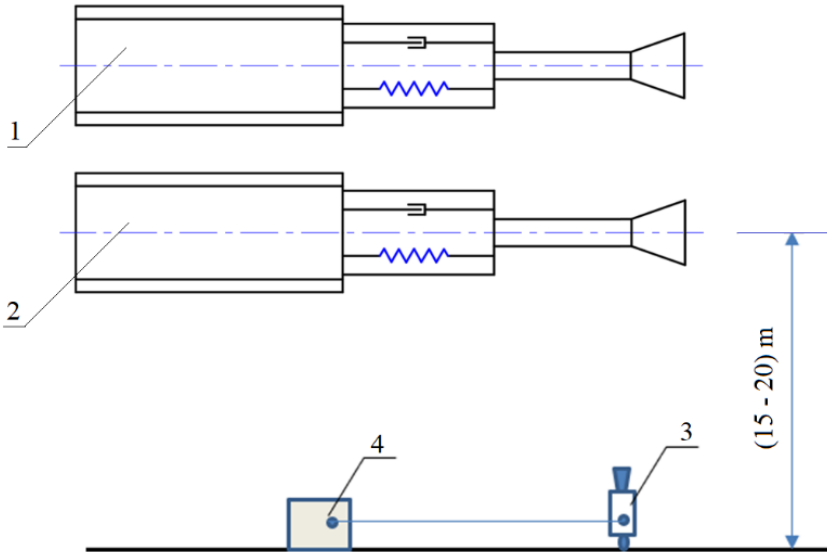


Fig. 9. Schema of the experimental setup
1, 2. Gun barrel; 3. High-speed camera; 4. Computer

The experiment has been performed under temperature of 30°C and humidity of 61% as Fig. 10.



Fig. 10. Position of camera SA1.1 measures vertical displacement

Measured data were processed using DASyLab analysing system. These results were compared with theoretical data by selecting the detected points which coincide with the measurement points. The parameters in experiment coincide with the parameters for theoretical calculations: the elevation and azimuth angle of gun on 2 shots was 0 degree. A comparison of calculation and experimental data are shown in Fig. 11 to Fig. 14.

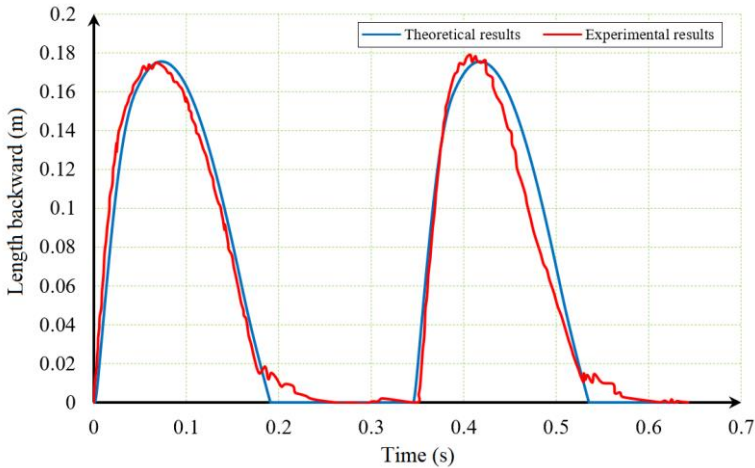


Fig. 11. Recoil length error of the right barrel

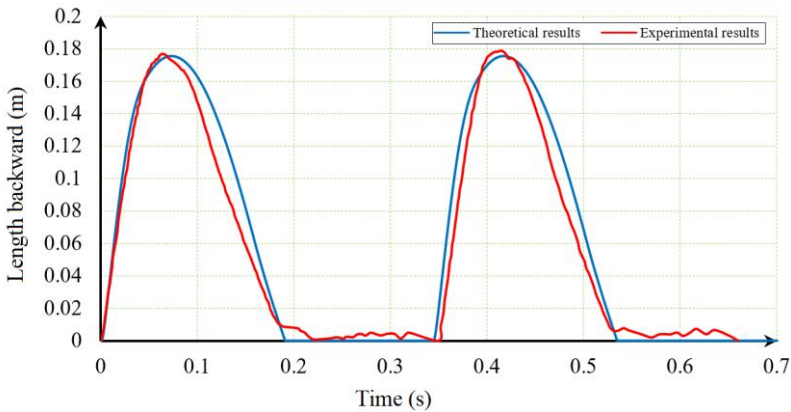


Fig. 12. Recoil length error of the left barrel

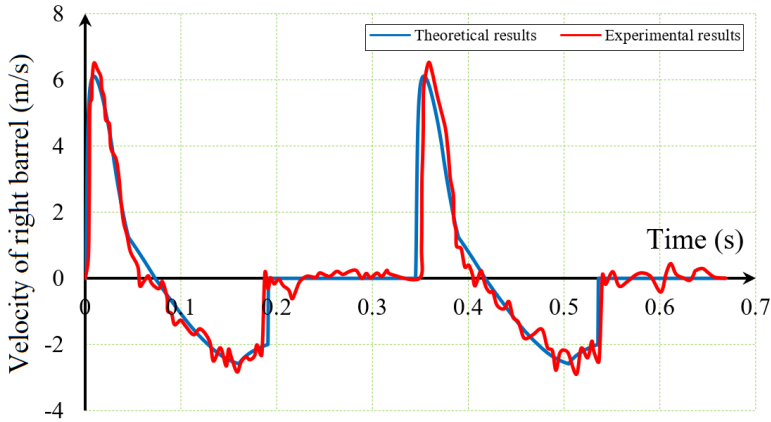


Fig. 13. Velocity error of the right barrel

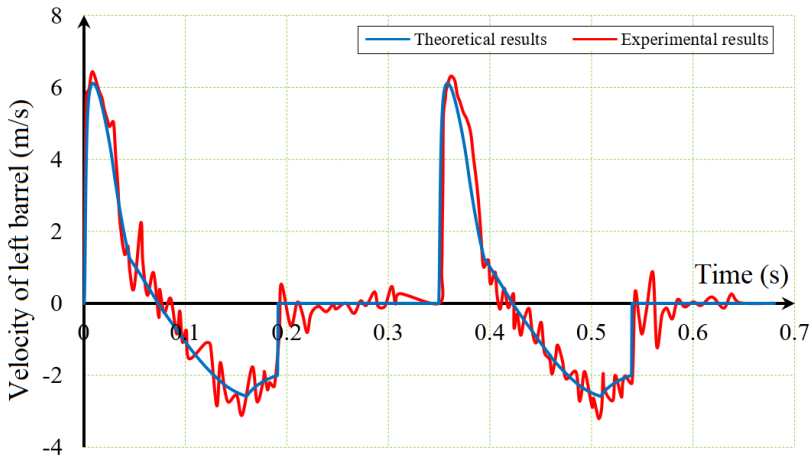


Fig. 14. Velocity error of the left barrel

4. CONCLUSIONS

This paper presents the setting up method of the motion equation for the automatic firing system based on the Lagrange equation of the second kind and experimental data. The comparisons show a very good agreement between the results of calculation and experimental results. Velocity and displacement of recoiling parts are calculated according to the math model and the experimental results are relatively similar. The maximum difference does not exceed 8.1%. The reason for discrepancy is the theoretical math model which has used several assumptions to simplify the calculation process. The results indicated that time error reaching maximum velocity is 0.03 s. The one functional cycle is theoretically 0.345 s, actually 0.3501 s. The measured data show that the recoil length and recoil velocity are different for both guns.

The reason is that two automatic firing systems have a completely independent structure, two barrels are not moved simultaneously while firing because two automatic firing systems are not absolutely the same in terms, for example the cartridges are not completely the same, characteristics of springs are different, etc. The results indicated that time displacement error of two automatic firing systems is 0.00206 (s).

The firing time of one shot is 0.345 s, equivalent to the theoretical rate of fire of 174 rds/min. The result is in accordance with the design document recorded in the manufacturer's documentation 160-180 rds/min. The results prove that the dynamic model for each automatic firing system ensures reliability and it can be used in the next researching and investigating of the 37 mm twin anti-aircraft gun type 65.

The comparison of results between theoretical calculation and experimental measurement shows the accuracy and suitability of the established model. The model can be applied solution to all types of an automatic firing system and the calculation results can be applied in the design or design optimisation of the 37 mm twin anti-aircraft gun type 65.

FUNDING

The work presented in this paper has been supported by the Weapon Technology Centre and Faculty of Weapons, Le Quy Don Technical University in Hanoi and by a research project of the Ministry of Defence and by the Research Support Project of the Department of weapon and ammunition, Faculty of Military Technology, University of Defence, Brno.

REFERENCES

- [1] U.S. Army Material Command Headquarters. 1970. *Engineering Design Handbook: Guns Series, Automatic Weapons*.
- [2] Huy Chuong Pham. 1998. *Textbook of structure and calculation on automatic firing system*. Hanoi, Vietnam: Military Technical Academy.
- [3] Vo Ng Anh. 1995. *Dynamics of automatic firing gun*. Hanoi, Vietnam: Military Technical Academy.
- [4] Doan Dao Van. 2011. *37 mm K65 anti-aircraft gun*. Hanoi, Vietnam: People Army Publishing House.
- [5] Quang M.A., Dao Van Doan. 2019. "Investigating influence of stiffness on vibration of elevating and traversing mechanisms of 37 mm twin anti-aircraft gun type 65", *Le Quy Don Technical University Journal of Science and Technique (LQDTU-JST)* 196 : 59-68.

- [6] Shabana A. Ahmed. 2005 *Dynamics of Multibody System* (Third Edition). Cambridge University Press.
- [7] Wittenburg Jens. 1977. *Dynamics of Systems of Rigid Bodies*. Vieweg+Teubner Verlag.
- [8] Nguyen N.D., V.T. Do. 1976. *Interior ballistics*. Hanoi, Vietnam: Military Technical Academy.



This article is an open access article distributed under terms and conditions of the Creative Commons Attribution-NonCommercial-NoDerivatives International 4.0 (CC BY-NC-ND 4.0) license (<https://creativecommons.org/licenses/by-nc-nd/4.0/>)